

DOI: 10.1002/open.201402068

Structural Elucidation of the O-Antigen Polysaccharide from *Escherichia coli* O181

Carolina Fontana,^[a] Andrej Weintraub,^[b] and Göran Widmalm^{*[a]}

Shiga-toxin-producing *Escherichia coli* (STEC) is an important pathogen associated to food-borne infection in humans; strains of *E. coli* O181, isolated from human cases of diarrhea, have been classified as belonging to this pathotype. Herein, the structure of the O-antigen polysaccharide (PS) from *E. coli* O181 has been investigated. The sugar analysis showed quinosamine (QuiN), glucosamine (GlcN), galactosamine (GalN), and glucose (Glc) as major components. Analysis of the high-resolution mass spectrum of the oligosaccharide (OS), obtained by dephosphorylation of the O-deacetylated PS with aqueous 48% hydrofluoric acid, revealed a pentasaccharide composed of two QuiNac, one GlcNac, one GalNac, and one Glc residue. The ¹H and ¹³C NMR chemical shift assignments of the OS were

carried out using 1D and 2D NMR experiments, and the OS was sequenced using a combination of tandem mass spectrometry (MS/MS) data and NMR ¹³C NMR glycosylation shifts. The structure of the native PS was determined using NMR spectroscopy, and it consists of branched pentasaccharide repeating units joined by phosphodiester linkages: →4)[α-L-QuipNac-(1→3)]-α-D-GalpNac6Ac-(1→6)-α-D-Glcp-(1→P-4)-α-L-QuipNac-(1→3)-β-D-GlcpNac-(1→; the O-acetyl groups represent 0.4 equivalents per repeating unit. Both the OS and PSs exhibit rare conformational behavior since two of the five anomeric proton resonances could only be observed at an elevated temperature.

Introduction

Escherichia coli strains are usually harmless microorganisms that inhabit the large intestine of humans and other warm-blooded animals, but some pathogenic strains are capable of causing intestinal diseases, urinary tract infections, sepsis, and meningitis.^[1] Among diarrheagenic *E. coli* strains, six different pathotypes can be distinguished: enteropathogenic *E. coli* (EPEC), enterohaemorrhagic *E. coli* (EHEC), enterotoxigenic *E. coli* (ETEC), enteroaggregative *E. coli* (EAEC), enteroinvasive *E. coli* (EIEC), and diffusely adherent *E. coli* (DAEC).^[2] Furthermore, Shiga-toxin-producing *E. coli* (STEC), also known as Verocytotoxin-producing *E. coli* (VTEC), are important human pathogens characterized by the production of one or more toxins of the Shiga toxin (Stx) family. The enterohaemorrhagic *E. coli* (EHEC) group mentioned above was originally defined as a subgroup of STEC associated with the appearance of haemorrhagic colitis (HC) and haemolytic uremic syndrome (HUS) in humans. However, the division between these two groups is

not very clear-cut, as the EHEC classification denotes a clinical connotation that is not implied in the STEC group.^[2,3]

The distinction of strains in different serogroups is of particular importance in epidemiological studies, and the O-antigen polysaccharide (PS) is one of the most important surface antigens used for classification.^[4] The *E. coli* serogroups are presently numbered from O1 to O187 according to the serological properties of their somatic antigen but, since seven of them have been removed (O31, O47, O67, O72, O93, O94, and O122), only 180 are currently in use.^[5–9] The ECODAB (*E. coli* O-antigen database) contains information about the structure, NMR chemical shifts, cross-reactivity, and information about glycosyltransferases (GTs) involved in the biosynthesis of many *E. coli* O-antigens.^[5,10]

E. coli O181 was recently reported and described as a Shiga-toxin-producing *E. coli* (STEC).^[11–14] Furthermore, serological cross-reactivity has been observed between a strain of the *E. coli* O181 serogroup and strains of the O3, O23, and O180 serogroups.^[11]

Results and Discussion

E. coli O181 was grown in a Luria–Bertini (LB) medium. The lipopolysaccharide (LPS) was isolated from the bacterial membrane by hot phenol/water extraction and delipidated under mild acid conditions to yield the polysaccharide, which was purified by size-exclusion chromatography. Sugar analysis of the polysaccharide revealed 2-amino-2,6-dideoxyglucose (quinosamine, QuiN), glucose (Glc), 2-amino-2-deoxyglucose (glucosamine, GlcN) and 2-amino-2-deoxygalactose (galactosa-

[a] Dr. C. Fontana, Prof. Dr. G. Widmalm
Arrhenius Laboratory, Department of Organic Chemistry
Stockholm University, S-106 91 Stockholm (Sweden)
E-mail: gw@organ.su.se

[b] Prof. Dr. A. Weintraub
Department of Laboratory Medicine, Division of Clinical Microbiology
Karolinska Institute, Karolinska University Hospital
S-141 86 Stockholm (Sweden)

© 2014 The Authors. Published by Wiley-VCH Verlag GmbH & Co. KGaA. This is an open access article under the terms of the Creative Commons Attribution-NonCommercial-NoDerivs License, which permits use and distribution in any medium, provided the original work is properly cited, the use is non-commercial and no modifications or adaptations are made.

mine, GalN) as the major components, in a ratio 1.5:0.7:1.9:1.0. Determination of the absolute configuration of the acetylated (+)-2-butyl glycosides of the PS by gas–liquid chromatography (GLC) showed L-QuiN, D-Glc, D-GlcN and D-GalN.

The ^1H NMR spectrum of the native PS showed six resonances (singlets) in the region between 1.97–2.12 ppm, attributed to O- and/or N-acetyl groups. After treatment with dilute aqueous sodium hydroxide only four methyl proton resonances (3H each) were observed in that region, which were attributed to N-acetyl groups. A similar O-deacetylated material was obtained after purification of the native PS by anion exchange chromatography followed by gel permeation chromatography (GPC). The anomeric region of the ^1H NMR spectrum of the GPC-purified material at different temperatures is shown in Figure 1. The monosaccharide residues were denoted A–E in

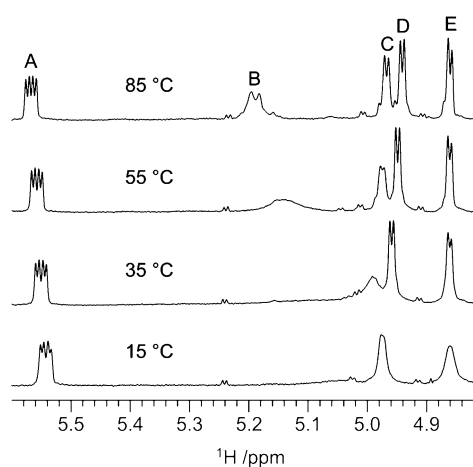


Figure 1. The anomeric region of the ^1H NMR spectrum of the O-deacetylated O-antigen PS of *E. coli* O181 recorded at different temperatures on a 600 MHz spectrometer. The spectrum on the bottom was acquired employing a diffusion-filtered experiment in order to remove the residual signal from the solvent.

order of decreasing chemical shifts of their anomeric protons. One should note that whereas only three anomeric resonances (from residues A, D, and E) are detected in the ^1H NMR spectrum recorded at 15 °C, an additional anomeric proton becomes noticeable at 55 °C (residue C), and a total of five anomeric protons are observed at 85 °C (residues A–E), indicating that the O-antigen PS is composed of pentasaccharide repeating units. In addition to the rare behavior of the anomeric resonances of residues B and C, when the temperature is increased from 5 to 85 °C, it is also observed that the anomeric resonance of residue D moves ~ 0.05 ppm upfield, and that of residue A moves ~ 0.03 ppm downfield, whereas the chemical shift of H1 of residue E is not significantly affected. The additional splitting of the anomeric resonance of residue A (Figure 1) indicated the presence of phosphorous. The ^{31}P NMR spectrum of the native PS showed a single resonance at a δ_{P} value of -2.18 ppm, indicating the presence of a phosphodiester linkage.^[15–17]

Structural analysis of the oligosaccharide

The O-deacetylated PS was subjected to dephosphorylation with aqueous 48% hydrogen fluoride and, after purification by size-exclusion chromatography, the resulting oligosaccharide material was analyzed by mass spectrometry (MS). High-resolution mass spectrometry (HRMS) using electrospray ionization (ESI) in the positive mode gave a spectrum of the underivatized oligosaccharide showing an intense peak at m/z 983.3800, corresponding to a compound of molecular formula $\text{C}_{38}\text{H}_{64}\text{N}_4\text{NaO}_{24}$ (calculated value 983.3803), which can be attributed to the pseudomolecular ion $[M + \text{Na}]^+$. This information, combined with the aforementioned sugar analysis of the native PS, is consistent with a pentasaccharide composed of two QuiNAC, one Glc, one GlcNAC, and one GalNAC residue. This is in agreement with the ^1H NMR spectrum of the O-deacetylated PS shown in Figure 1, where five anomeric resonances are observed. The ^1H NMR spectrum of the dephosphorylated material (Figure 2a) shows a mixture of two pentasaccharides that differ from each other in the anomeric configuration of the monosaccharide located at their reducing end (the α - and β -anomers, in a 2:3 ratio, are denoted A' and A' in Figure 2a, respectively).

The ^1H and ^{13}C chemical shift assignments were carried out using ^1H and ^{13}C NMR spectroscopy (Figure 2a,b), multiplicity-edited ^1H , ^{13}C -heteronuclear single quantum coherence (^1H , ^{13}C -HSQC) (Figure 2c–e) spectroscopy, ^1H , ^{13}C -heteronuclear 2-bond correlation (^1H , ^{13}C -H2BC) spectroscopy, ^1H , ^{13}C -heteronuclear multiple bond correlation (^1H , ^{13}C -HMBC) spectroscopy, and ^1H , ^1H -total correlation spectroscopy (^1H , ^1H -TOCSY) employing different mixing times, and the assignments are compiled in Table 1. The resonances from the major pentasaccharide component are denoted with primed characters, whereas those of the minor component are denoted with double primed characters. All of the H1 and C1 resonances have chemical shifts typical of hexopyranosyl residues. The H6 resonances of C', C'', D' and D'' are present between 1.244–1.314 ppm and the C6 resonances are found between 17.15–17.37 ppm, indicating that these are 6-deoxy-hexoses (L-QuipNAC). The C2 resonances of residues B', B'', E' and E'' occur between 57.45 and 49.99 ppm, indicating that these are nitrogen-bearing carbons, and thus the N-acetyl hexosamine residues. From the correlation patterns observed in the ^1H , ^1H -TOCSY spectra it was deduced that residue B' and B'' have the *gluco*-configuration and residues E' and E'' have the *galacto*-configuration (i.e., in the ^1H , ^1H -TOCSY spectrum with the longest mixing time, all of the protons in the spin system can be traced from H1 of residues B' and B'' to H6, but only those protons up to H4 can be traced from the anomeric protons of residues E' and E'', indicating a small $^3J_{\text{H4,H5}}$ value in the latter case). Thus, residues B' and B'' are D-Glc pNAC and residues E' and E'' are D-Gal pNAC. Therefore, residues A' and A'' are D-Glc p.

Residues A'', C', C'', D', D'', E', and E'' are sugars with the α -anomeric configuration since the $^3J_{\text{H1,H2}}$ couplings are 3.6–3.9 Hz, whereas residue A' has the β -anomeric configuration as the $^3J_{\text{H1,H2}}$ coupling is 7.9 Hz. Notably, it was observed that the H1, H2, H3, C1, and C2 resonances of residue B are considera-

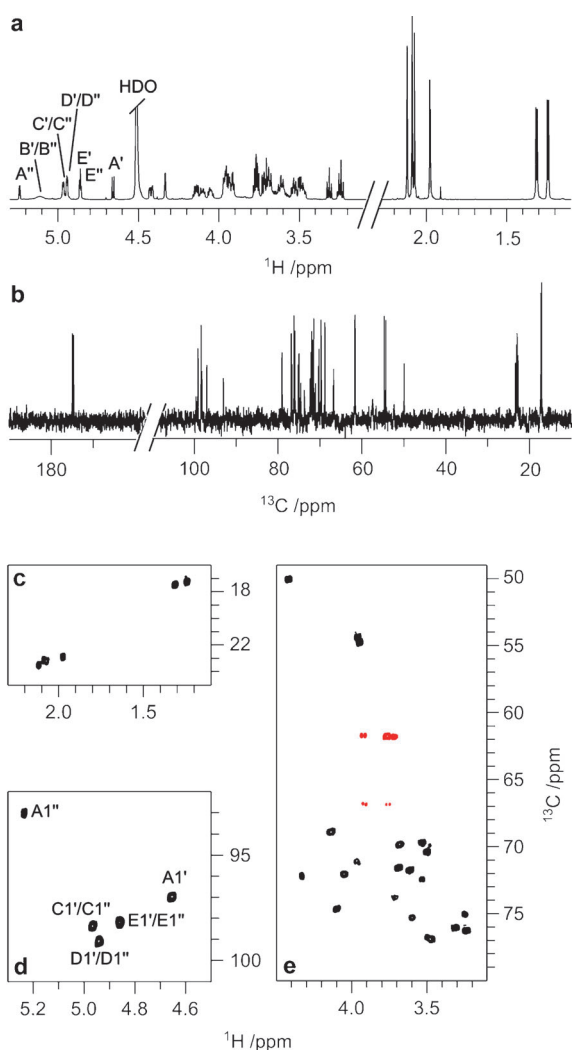


Figure 2. a) ^1H and b) ^{13}C NMR spectra of the pentasaccharides obtained by dephosphorylation of the O-deacetylated O-antigen PS of *E. coli* O181; c–e) selected regions of the multiplicity-edited ^1H , ^{13}C -HSQC spectrum showing the methyl groups (c) and anomeric region (d), as well as the region for the resonances of ring atoms and hydroxymethyl groups (e), where the latter appear in red. All spectra were recorded at 49 °C on a 700 MHz spectrometer. At this temperature, the B1, B2, and B3 resonances are too broad to be observed in the multiplicity-edited ^1H , ^{13}C -HSQC NMR spectrum.

bly broadened at 49 °C, and thus the respective cross-peaks are not observed in the ^1H , ^{13}C -HSQC spectrum (Figure 2d–e). This indicates that the rare behavior observed in the PS is also present in the oligosaccharide. As a consequence of the broadening of the H1 resonance of residues B' and B'' it was not possible to extract the $^3J_{\text{H1,H2}}$ coupling, but the characteristic chemical shift of C5 (76.89 ppm) suggests that this monosaccharide is β -linked (i.e. the chemical shift of C5 in the α - and β -anomeric forms of GlcpNac are typically 72.5 and 76.8 ppm, respectively).^[19]

The substitution positions for the sugar residues in the oligosaccharide were identified from ^{13}C NMR glycosylation shifts.^[19–21] Since residues A' and A'' do not show any significant glycosylation shift for C1, these residues are located at the reducing end of the respective pentasaccharides; the gly-

cosylation shifts $\Delta\delta_{\text{C6,A}'} = 4.94$ and $\Delta\delta_{\text{C6,A}''} = 5.04$ show that they are $\rightarrow 6$ - β -D-Glcp and $\rightarrow 6$ - α -D-Glcp, respectively. Residues B' and B'' are $\rightarrow 3$ - β -D-GlcpNac-(1 \rightarrow) since $\Delta\delta_{\text{C3}} = 4.27$, and residues E' and E'' are $\rightarrow 3,4$ - α -D-GalpNac-(1 \rightarrow) since $\Delta\delta_{\text{C3}} = 6.22$ and $\Delta\delta_{\text{C4}} = 2.58$. On the other hand, residues C', C'', D', and D'' do not show any significant glycosylation shifts for the C2–C6 atoms and thus are terminal non-reducing α -L-QuipNac-(1 \rightarrow) residues.

Information about the monosaccharide sequence in the oligosaccharide was obtained by MS/MS in both the positive and negative modes from the precursor pseudomolecular ions m/z 983.4 (Figure 3a) and 959.4 (Figure 3b), respectively, which produced the corresponding daughter ions via A₁-, B-, C- and E-type cleavages.^[18] The daughter ion m/z 796.3 (Figure 3a) is consistent with the loss of a terminal QuiNac residue (residue C'/C'' or D'/D'' in Table 1). Furthermore, the daughter ion m/z 413.2 corresponds to a QuiNac-HexNac fragment obtained via an A₁-type cleavage, whereas the daughter ion m/z 593.2 corresponds to the loss of a QuiNac-HexNac moiety (cf. Figure 3a). According to these fragmentation patterns, the aforementioned HexNac residue is monosubstituted and thus can be assigned to the GlcNac residue (B'/B'') of Table 1. From the NMR analysis it was revealed that a 6-substituted Glc residue (A'/A'') is located at the reducing end of the oligosaccharide, which is consistent with the daughter ion m/z 839.3 observed in the spectrum of Figure 3b. Furthermore, since both QuiNac residues are located at terminal non-reducing ends (cf. Table 1) the fragment m/z 593.2 in Figure 3a can be assigned to a QuiNac-GalNac-Glc moiety, where QuiNac is either residue C'/C'' or D'/D'', GalNac is residue E'/E'', and Glc is residue A'/A''. Due to the broadening of the resonances of residue B'/B'', the inter-residue correlations involving these monosaccharides could not be observed in the ^1H , ^{13}C -HMBC spectrum. However, unambiguous correlations were observed from the anomeric protons of residues D'/D'' to C3 of residue E'/E'', and from the anomeric proton of residues E'/E'' to C6 of residues A'/A''. Thus, the sequence in the oligosaccharide is as defined in Figure 3. Having considered this, the fragments m/z 592.2 and 202.2, observed in the MS/MS spectrum of Figure 3b, are attributed to a β -elimination processes taking place at the C3 position of a 3-substituted HexNac residue after a C-type cleavage of the HexNac glycosidic bond.^[22]

Structural analysis of the O-deacetylated and native PSs

According to the aforementioned results, the PS is composed of pentasaccharide repeating units joined by phosphodiester linkages. The multiplicity-edited ^1H , ^{13}C -HSQC spectrum of the O-deacetylated PS recorded at 85 °C is shown in Figure 4a–c, and all cross-peaks are clearly observed at this temperature (cf. Figure 1a top). Five anomeric resonances are observed in the region for the hexopyranosyl residues (Figure 4a) whereas six cross-peaks are observed in the region for the resonances of methyl groups (two from H6/C6 of 6-deoxy sugars and four from N-acetyl groups, Figure 4c). The ^1H and ^{13}C NMR chemical shift assignments of the O-deacetylated PS were carried out at

Table 1. ^1H and ^{13}C NMR chemical shift assignments of the oligosaccharide obtained by dephosphorylation of the O-deacetylated O-antigen polysaccharide from *E. coli* O181 at 49 °C.

Sugar residue ^[a]		$^1\text{H}/^{13}\text{C}$ NMR δ [ppm]							
		1	2	3	4	5	6	Me	CO
→6)-β-D-Glcp	A'	4.658 [7.9]	3.251	~3.489	~3.489	3.600	3.760, 3.916	–	–
		(0.02)	(0.00)	(–0.01)	(0.07)	(0.14)	–	–	–
		96.99	75.03	76.72	70.40	75.24	66.78	–	–
→3)-β-D-GlcpNAC-(1→	B'	(0.15)	(–0.17)	(–0.04)	(–0.31)	(–1.52)	(4.94)	–	–
		~5.113 ^[b]	~3.627 ^[b]	~3.915 ^[b]	3.536	3.472	3.764, 3.921	2.120	–
		(0.39)	(–0.02)	(0.36)	(0.08)	(0.01)	–	(0.06)	–
α-L-QuipNAC-(1→	C'	~99.53 ^[b]	~57.45 ^[b]	79.08	69.70	76.89	61.66	23.42	174.95
		(3.68)	(–0.41)	(4.27)	(–1.36)	(0.07)	(–0.19)	(0.32)	(–0.54)
		4.969 [3.6]	3.949	3.689	3.240	4.139	1.244	2.088	–
α-L-QuipNAC-(1→	D'	(–0.18)	(0.09)	(–0.01)	(–0.20)	(0.24)	(–0.05)	(0.03)	–
		98.36	54.71	71.51	76.22	68.85	17.15	23.02	174.95
		(6.69)	(–0.41)	(0.02)	(–0.29)	(0.56)	(–0.31)	(0.15)	(–0.18)
α-L-QuipNAC-(1→	D''	4.944 [3.9]	3.962	3.614	3.313	3.682	1.314	2.073	–
		(–0.21)	(0.10)	(–0.09)	(0.05)	(–0.22)	(0.02)	(0.01)	–
		99.09	54.31	71.73	76.01	69.81	17.37	23.14	174.65
→3,4)-α-D-GalpNAC-(1→	E'	(7.40)	(–0.81)	(0.24)	(–0.50)	(1.52)	(–0.09)	(0.27)	(–0.48)
		4.865 [3.8]	4.423	4.095	4.333	4.048	3.719, 3.773	1.980	–
		(–0.42)	(0.23)	(0.15)	(0.28)	(–0.08)	–	(–0.08)	–
→6)-α-D-Glcp	A''	98.14	49.99	74.62	72.14	72.01	61.74	22.81	174.65
		(6.19)	(–1.17)	(6.22)	(2.58)	(0.65)	(–0.37)	(–0.10)	(–0.78)
		5.239 [3.8]	3.533	3.717	3.501	3.698	3.701, 3.953	–	–
→3)-β-D-GlcpNAC-(1→	B''	(0.01)	(–0.01)	(0.00)	(0.08)	(–0.14)	–	–	–
		93.03	72.38	73.78	70.29	71.10	66.88	–	–
		(0.04)	(–0.09)	(0.00)	(–0.42)	(–1.27)	(5.04)	–	–
→3)-β-D-GlcpNAC-(1→	B''	~5.113 ^[b]	~3.627 ^[b]	~3.915 ^[b]	3.536	3.472	3.764, 3.921	2.120	–
		(0.39)	(–0.02)	(0.36)	(0.08)	(0.01)	–	(0.06)	–
		~99.53 ^[b]	~57.45 ^[b]	79.08	69.70	76.89	61.66	23.42	174.95
α-L-QuipNAC-(1→	C''	(3.68)	(–0.41)	(4.27)	(–1.36)	(0.07)	(–0.19)	(0.32)	(–0.54)
		4.969 [3.6]	3.949	3.689	3.240	4.139	1.244	2.088	–
		(–0.18)	(0.09)	(–0.01)	(–0.20)	(0.24)	(–0.05)	(0.03)	–
α-L-QuipNAC-(1→	D''	98.36	54.71	71.51	76.22	68.85	17.15	23.02	174.95
		(6.69)	(–0.41)	(0.02)	(–0.29)	(0.56)	(–0.31)	(0.15)	(–0.18)
		4.947 [3.9]	3.962	3.614	3.313	3.682	1.314	2.073	–
α-L-QuipNAC-(1→	D''	(–0.20)	(0.10)	(–0.09)	(0.05)	(–0.22)	(0.02)	(0.01)	–
		99.07	54.31	71.73	76.01	69.81	17.37	23.14	174.65
		(7.42)	(–0.81)	(0.24)	(–0.50)	(1.52)	(–0.09)	(0.27)	(–0.48)
→3,4)-α-D-GalpNAC-(1→	E''	4.859 [3.8]	4.420	4.104	4.333	4.048	3.719, 3.773	1.975	–
		(–0.42)	(0.23)	(0.15)	(0.28)	(–0.08)	–	(–0.09)	–
		98.24	50.02	74.62	72.14	72.01	61.74	22.80	174.65
		(6.29)	(–1.14)	(6.22)	(2.58)	(0.65)	(–0.37)	(–0.11)	(–0.78)

[a] The ratio between the reducing end anomeric forms of the oligosaccharide, denoted with primed and doubled primed characters, is 3:2. Chemical shift differences ($\Delta\delta$) as compared with the corresponding monosaccharides^[19,21] are given in parentheses. $^3J_{\text{H}_1,\text{H}_2}$ values are given in Hz and are in square brackets. [b] Broad peak.

70 °C using 1D and 2D NMR experiments, and they are compiled in Table 2 (denoted with non-primed characters).

Residues A, C, D, and E are α -linked since $^3J_{\text{H}_1,\text{H}_2}$ are 3.5–4.0 Hz and $^1J_{\text{C}_1,\text{H}_1}$ are 172–174 Hz, and residue B is β -linked since $^3J_{\text{H}_1,\text{H}_2}$ is 8.0 Hz and $^1J_{\text{C}_1,\text{H}_1}$ is 162 Hz.^[23] Analogously to what was observed in the aforementioned oligosaccharide, in the O-deacetylated PS residue B is →3)-β-D-GlcpNAC-(1→ since $\Delta\delta_{\text{C}_3}$ is 4.33, residue E is →3,4)-α-D-GalpNAC-(1→ since $\Delta\delta_{\text{C}_3}$ is 6.35 and $\Delta\delta_{\text{C}_4}$ is 2.55, and residue D is a terminal non-reducing α-L-QuipNAC-(1→ since no significant glycosylation shifts were observed for the C2–C6 atoms. However, in this case, residue A is not a reducing end monosaccharide as $\Delta\delta_{\text{C}_1}$ is 3.07, and it is →6)-α-D-Glcp-(1→ since $\Delta\delta_{\text{C}_6}$ is 4.69; and residue C is →4)-α-L-QuipNAC-(1→ since $\Delta\delta_{\text{C}_4}$ is 4.73. The multiplicity-edited $^1\text{H},^{13}\text{C}$ -HSQC spectrum of the native PS (Figure 4d–f) showed

a conspicuous cross-peak at $\delta_{\text{H}}/\delta_{\text{C}} = 2.128/21.06$ (Figure 4f), attributed to a methyl group of an O-acetyl moiety. Integration of the proton methyl resonances of the O- and N-acetyl groups in the ^1H NMR spectrum revealed that the native PS contains ~0.4 equivalents of the O-acetyl group per repeating unit. Comparison of the multiplicity-edited $^1\text{H},^{13}\text{C}$ -HSQC spectrum of the native PS with that of the O-deacetylated PS allowed identification of the resonances from the non-O-acetylated repeating units. In addition, two monosaccharide spin systems were also identified using 1D and 2D NMR experiments, and denoted A''' and E''' in Table 2. The former showed a set of signals similar to that of residue A, but with slightly altered chemical shifts, whereas the latter showed similar H1–H4 and C1–C4 resonances to that of residue E, but with significant altered H5/C5 and H6/C6 chemical shifts (annotated in Fig-

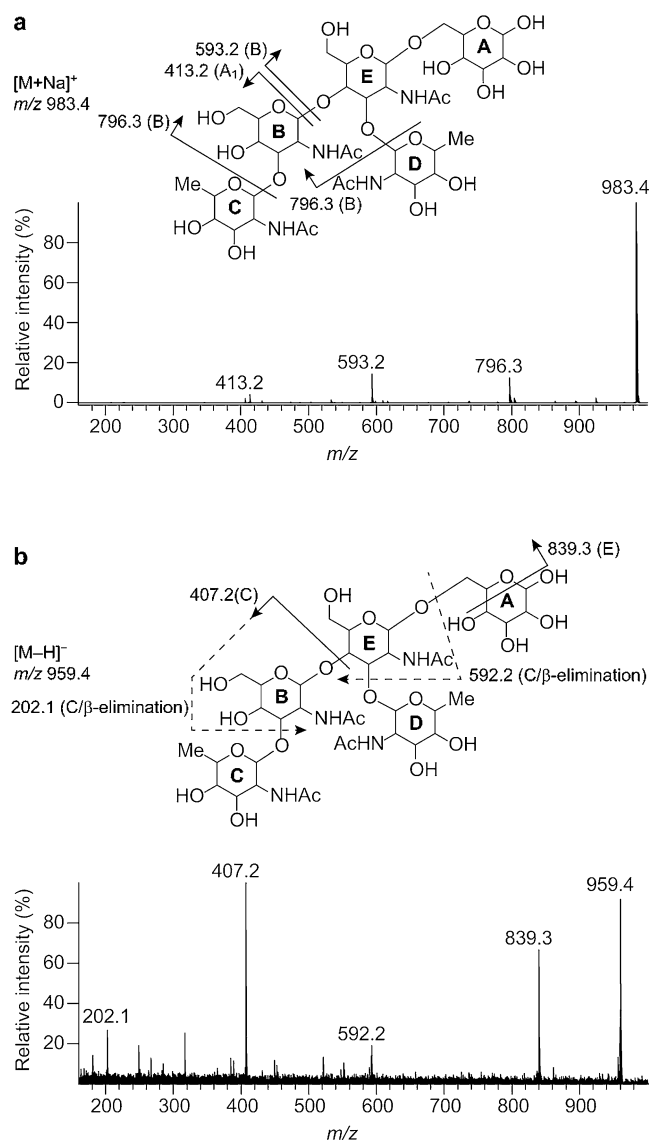


Figure 3. The MS/MS spectra of the pentasaccharide compound obtained after cleavage of the phosphodiester groups of the O-deacetylated PS of *E. coli* O181: a) pseudomolecular $[M+Na]^+$ ion m/z 983.4 recorded in positive mode; b) pseudomolecular $[M-H]^-$ ion m/z 959.4 recorded in negative mode. The detected ions are shown in the structure located on the top of each spectrum, and the fragmentation pathway^[18] is indicated in parentheses. Double fragmentations are indicated with dashed lines. The monosaccharide residues are denoted A–E according to the nomenclature used in Table 1 and correspond to the respective primed or double primed characters.

ure 4e) that could be attributed to perturbations due to 6-O-acetylation since $\Delta\delta_{C_6,E''}$ is 3.05.^[24,25]

Assignment of the amide protons in the native PS were carried out in a 95:5 H₂O/D₂O mixture at 49 °C using ¹H,¹H-TOCSY experiments. In the ¹H,¹H-TOCSY spectrum recorded with a mixing time of 100 ms, all of the resonances from H1 to H6 could be traced from the NH protons of residues B, C, and D, whereas only those resonances from H1 to H4 were traced from the NH protons of residues E and E'' (Figure 5 a–b). Furthermore, the methyl groups from the N-acetyl groups were successfully assigned to the respective monosaccharides using

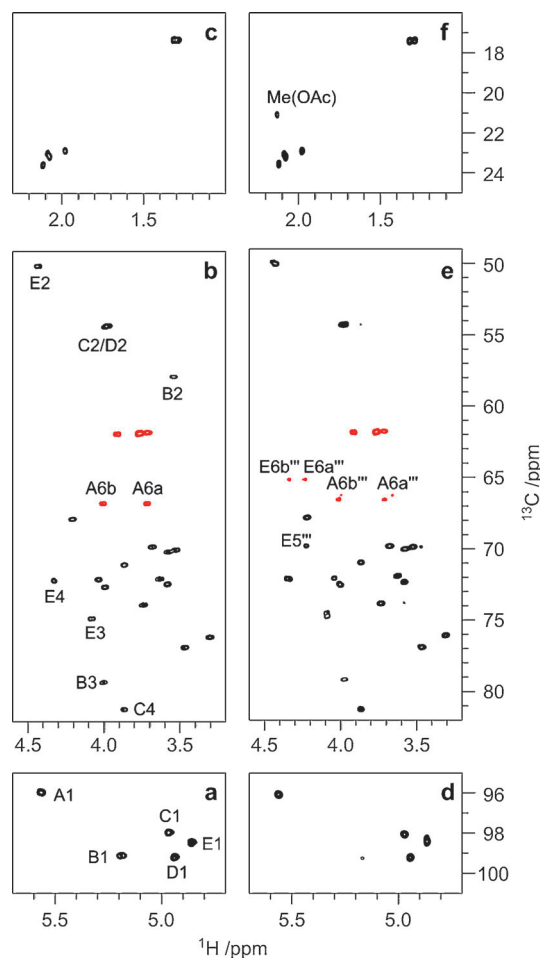


Figure 4. Comparison of the multiplicity-edited ¹H,¹³C-HSQC spectra of the O-deacetylated and native O-antigen PSs of *E. coli* O181 (left and right, respectively), showing the anomeric region (a and d), the region for the ring atoms, nitrogen-bearing carbons (~50–60 ppm), and hydroxymethyl groups (in which the cross-peaks from the latter appear in red at ~61–67 ppm) (b and e), and the region for the methyl groups (c and f). The spectrum on the left was recorded at 85 °C on a 600 MHz spectrometer, whereas the spectrum on the right was recorded at 70 °C on a 700 MHz spectrometer. In the spectrum of the O-deacetylated PS (left) resonances from anomeric and substitution positions are annotated. In panel e, the cross-peaks of the native PS that have altered chemical shifts due to O-acetylation (with respect to the spectrum on the left) are indicated, and the cross-peak from the methyl moiety of the O-acetyl group is annotated in panel f. Note that the H2–C2 correlation of residue B is not shown since its intensity is too low at this plot level.

¹H,¹H-NOESY correlations from the respective NH protons (Figure 5 c). The carbonyl groups of O- and N-acetyl groups in the native PS were assigned via two-bond proton–carbon correlations from the respective methyl protons using a band-selective constant-time ¹H,¹³C-HMBC spectrum recorded with a selective ¹³C refocusing pulse applied at the center of the carbonyl region. The location of the O-acetyl group was confirmed by a correlation from the respective carbonyl carbon ($\delta_{CO} = 174.77$ ppm) to protons at 4.237 and 4.340 ppm (H6 protons in residue E'''), in addition to a correlation to the methyl protons at 2.128 ppm.

The location of the phosphorous atom was confirmed using ¹H–³¹P correlations from 2D heteronuclear experiments. In

Table 2. ^1H and ^{13}C NMR chemical shift assignments of the O-antigen polysaccharide from *E. coli* O181 at 70 °C.

Sugar residue		$^1\text{H}/^{13}\text{C}$ NMR δ [ppm] ^[a]						Me[NAc]	CO[NAc]	NH ^[c]
		1 ^[b]	2	3	4	5	6			
→6)-α-D-Glcp-(1→P ^[d]	A	5.562 ^[e] [3.5]	3.584	3.727	3.584	3.995	3.708, 4.009	–	–	–
		(0.33)	(0.04)	(0.01)	(0.16)	(0.16)	–	–	–	–
		96.06 ^[f] {174}	72.31 ^[g]	73.79	70.02	72.57	66.53	–	–	–
→3)-β-D-GlcpNAc-(1→	B	5.165 [8.0]	3.567	3.972	3.525	3.472	3.762, 3.916	2.118	–	8.201
		(0.45)	(–0.08)	(0.41)	(0.06)	(0.01)	–	(0.06)	–	–
		99.28 {162}	57.73	79.14	69.87	76.87	61.80	23.53	174.90	–
→4)-α-L-QuipNAc-(1→	C	4.970 [3.9]	3.988	3.865	3.863	4.218	1.286	2.085	–	7.980
		(–0.18)	(0.13)	(0.17)	(0.60)	(0.32)	(0.00)	(0.02)	–	–
		98.04 {172}	54.28	70.96	81.24 ^[h]	67.80 ^[i]	17.34	23.03	174.79	–
α-L-QuipNAc-(1→	D	4.945 [4.0]	3.968	3.626	3.306	3.683	1.317	2.076	–	7.424
		(–0.21)	(0.11)	(–0.07)	(0.05)	(–0.22)	(0.03)	(0.02)	–	–
		99.20 {172}	54.28	71.91	76.07	69.80	17.38	23.19	174.61	–
→3,4)-α-D-GalpNAc-(1→	E	4.861 [3.5]	4.427	4.085	4.334	4.044	3.720, 3.768	1.980	–	8.002
		(–0.42)	(0.24)	(0.14)	(0.28)	(–0.09)	–	(–0.08)	–	–
		98.47 {173}	50.06	74.75	72.11	72.06	61.75	22.89	174.55	–
→6)-α-D-Glcp-(1→	A'''	5.562	3.584	3.727	3.584	4.009	3.664, 4.000	–	–	–
		(0.33)	(0.04)	(0.01)	(0.16)	(0.17)	–	–	–	–
		96.06	72.31	73.79	70.02	72.41	66.24	–	–	–
→3,4)-α-D-GalpNAc6Ac-(1→ ^[j]	E'''	4.865	4.447	4.091	4.356	4.224	4.237, 4.340	1.976	–	8.025
		(–0.42)	(0.26)	(0.14)	(0.31)	(0.09)	–	(–0.08)	–	–
		98.31	49.90	74.47	72.09	69.80	65.16	22.89	174.58	–
		(6.36)	(–1.26)	(6.07)	(2.53)	(–1.56)	(3.05)	(–0.02)	(–0.88)	–

[a] The ^1H and ^{13}C NMR chemical shifts of residues A, B, C, D, and E were obtained from the O-deacetylated PS, whereas those of A''' and E''' were obtained from the native PS. The native PS contains ~0.4 equiv of the O-acetyl group per repeating unit. Chemical shift differences ($\Delta\delta$) as compared with the corresponding monosaccharides^[19,21] are given in parentheses. [b] $^3J_{\text{H}_1, \text{H}_2}$ and $^1J_{\text{H}_1, \text{C}_1}$ values are given in Hz in square brackets and braces, respectively. [c] Chemical shifts at 49 °C. [d] δ_{P} at 49 °C is –2.18 ppm. [e] $^3J_{\text{PH}} = 7.2$ Hz. [f] $^2J_{\text{PC}} = 6.3$ Hz. [g] $^3J_{\text{BC}} = 7.6$ Hz. [h] $^2J_{\text{PC}} = 6.6$ Hz. [i] $^3J_{\text{PC}} = 6.2$ Hz. [j] The O-acetyl group resonances are at $\delta_{\text{H}} = 2.128$ ppm (Me), and $\delta_{\text{C}} = 21.06$ ppm (Me) and 174.77 ppm (CO).

both the $^1\text{H}, ^{31}\text{P}$ -HMBC and $^1\text{H}, ^{31}\text{P}$ -hetero-TOCSY spectrum recorded with a mixing time of 20 ms, the strongest correlations from the phosphorus resonance at –2.18 ppm were observed to H1 in residue A and H4/H3 of residue C. Further correlations from the phosphorous atom to all H1 to H6 protons in residues A and C could be observed in the $^1\text{H}, ^{31}\text{P}$ -hetero-TOCSY spectrum recorded with a mixing time of 50 ms (Figure 5 e–g). Thus, considering the glycosylation shift of C4 in residue C ($\Delta\delta_{\text{C}_4} = 4.73$), it is concluded that the native PS consists of branched pentasaccharide repeating units joined by phosphodiester linkages between O1 of residue A and O4 of residue C. Furthermore, inter-residue $^1\text{H}, ^1\text{H}$ -NOESY correlations were observed from the anomeric protons of residues B, C, D, E, and E''' to the protons at the respective substitution positions (Figure 6 a–b), which define the sequence of sugar residues in the repeating unit as previously deduced for the oligosaccharide material (cf. Figure 3). Additional inter-residue correlations were also observed in the $^1\text{H}, ^1\text{H}$ -NOESY spectrum between H1 in residue B and H3 and H5 in residue D (Figure 6 b), as well as from the methyl protons of the N-acetyl group in residue B to H2 in residue E/E''' and H1 in residue C, and from the methyl protons of the N-acetyl group in residues E/E''' to H1 in residue D. These results are also consistent with the correlations observed in the $^1\text{H}, ^1\text{H}$ -NOESY spectrum recorded in

95:5 H₂O:D₂O mixture from the amide proton in residue B to H2 in residue E/E''' and H1 in residue C, and from the amide protons of residues E/E''' to H1 in residue D (Figure 5 d). The aforementioned $^1\text{H}, ^1\text{H}$ -NOESY correlations are illustrated in the schematic representation of a part of the O-antigen repeating unit shown in Figure 6 c.

The results from the $^1\text{H}, ^{13}\text{C}$ -HMBC spectrum (Table 3) were in agreement with those of the $^1\text{H}, ^1\text{H}$ -NOESY experiment, and consequently the repeating unit of the native O-antigen PS from *E. coli* O181 is as shown in Figure 7. The O-deacetylated O-antigen PS of *E. coli* O181 is then remarkably similar to that of the *Proteus vulgaris* O1,^[26,27] with the only difference being the presence of a →6)-α-D-Glcp-(1→ residue in the former instead of the →4)-α-D-Galp-(1→ residue of the latter.

The broadening of the C1, C2, H1, H2, H3, and N-acetyl methyl proton resonances in residue B at 35 °C indicates a dynamic behavior of the β-D-GlcpNAc residue probably affecting the conformation of the corresponding atoms in this residue, and thus the conformation of the pyranose ring. The H1 resonance of residue C is also broadened at that temperature, indicating that the conformational behavior of residue B also affects the α-(1→3) glycosidic linkage between residues C and B. Even though the D-GlcpNAc residues usually adopt a stable $^4\text{C}_1$ conformation, it has been recently reported that some oligo-

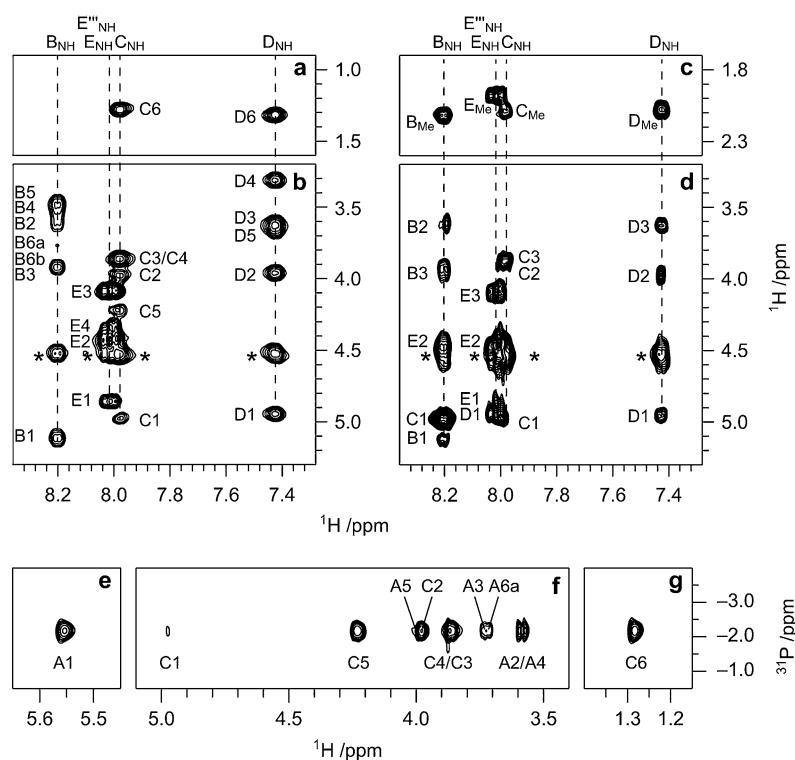


Figure 5. Selected regions of the a–b) $^1\text{H}, ^1\text{H}$ -TOCSY and c–d) $^1\text{H}, ^1\text{H}$ -NOESY spectra of the native PS of *E. coli* O181 showing correlations from the NH protons. Both spectra were recorded in a 95:5 $\text{H}_2\text{O}/\text{D}_2\text{O}$ mixture, using mixing times of 100 ms. e–g) $^1\text{H}, ^{31}\text{P}$ -hetero-TOCSY spectrum of the same PS recorded in D_2O , using a mixing time of 50 ms. All spectra were recorded at 49 °C. The cross-peaks denoted by an asterisk originate from correlations to the water peak.

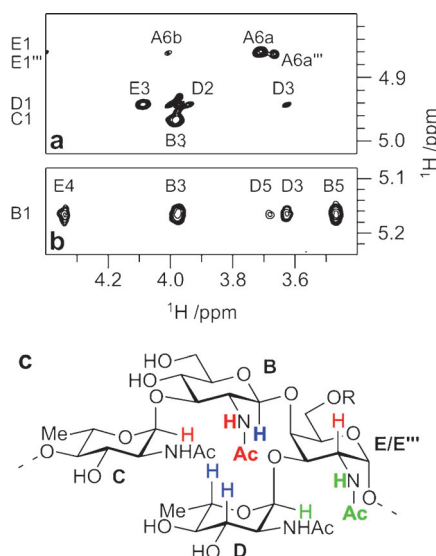


Figure 6. Selected regions of the $^1\text{H}, ^1\text{H}$ -NOESY spectrum ($\tau_{\text{mix}} = 100$ ms) of the native O-antigen PS of *E. coli* O181 (recorded in D_2O and at 70 °C) showing intra- and inter-residue correlations from the anomeric protons of residues C, D, E, and E''' (a) and B (b). Schematic representation of part of the O-antigen repeating unit showing some key $^1\text{H}, ^1\text{H}$ -NOESY inter-residue correlations (c); the correlations are observed from the protons indicated in bold to the other protons sharing the same color. Residues E and E''' differ by the R substituent that is H or Ac, respectively.

saccharides containing these kinds of residues can adopt unusual conformations.^[28,29] In the case of the O-specific chain of

E. coli O181, the β -D-GlcNAc residue is substituted at O3, and the double substitution of residue E (at the O3 and O4 positions) makes this region of the molecule considerably crowded (which is evidenced by the NOE correlations shown in red and green in Figure 6c).

Conclusion

The O-antigen polysaccharide (PS) of *E. coli* O181 consists of branched pentasaccharide repeating units joined by phosphodiester linkages. This PS shares a tetrasaccharide moiety with the O-antigen of *Proteus vulgaris* O1. The broadening of some key resonances in the ^1H and ^{13}C NMR spectra recorded at temperatures below 85 °C suggests an unusual conformational behavior of the β -D-GlcNAc residue. Further studies are required to unveil the dynamics behind these observations.

Table 3. Inter-residue correlations from $^1\text{H}, ^{13}\text{C}$ -HMBC, $^1\text{H}, ^{31}\text{P}$ -HMBC, and $^1\text{H}, ^1\text{H}$ -NOESY NMR spectra of the native O-antigen PS from *E. coli* O181.

Residue	Atom	Residue	$^1\text{H}, \text{X}$ -HMBC ^[a]	$^1\text{H}, ^1\text{H}$ -NOESY
A	P	A	H1, H2	–
A	P	C	H2, H3&H4, ^[b] H5	–
B	H1	D	–	H3, H5
B	H1	E	–	H4
B	C1	E	H4	–
C	H1	B	C3	H3, NH, Me
D	H1	E	C3	H3, NH, Me
D	C1	E	H3	–
E	H1	A	C6	H6a, H6b
E	H2	B	–	NH, Me
E	C1	A	H6a, H6b	–
E'''	H1	A'''	C6	H6a

[a] The X refers either to ^{13}C or ^{31}P according to the atom specified. [b] In residue C, the strongest cross-peak was observed for the overlapping resonances of H3 and H4.

Experimental Section

Bacterial strain, conditions of growth, and preparation of the native polysaccharide

The strain of *E. coli* O181 was obtained from the International Escherichia and Klebsiella Center (World Health Organization), Statens Serum Institute, Copenhagen, Denmark. The bacteria were grown, the LPS isolated, and the delipidated PS purified as previously described.^[31] The native PS was purified on an ÄKTA purifier system

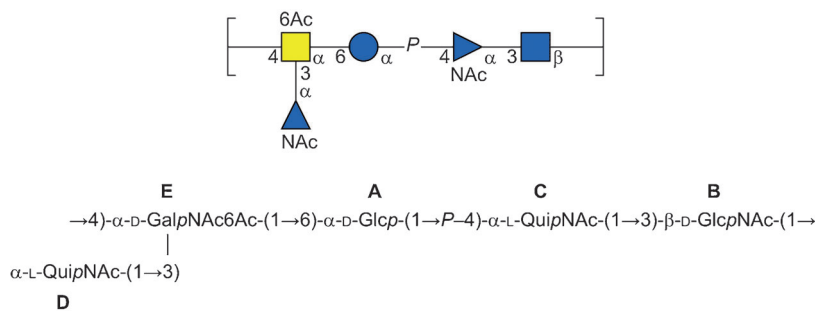


Figure 7. Structure of the repeating unit of the O-antigen PS of *E. coli* O181 in Consortium for Functional Genomics (CFG) notation^[30] (top) and standard nomenclature (bottom). The O-acetyl groups represent 0.4 equiv per repeating unit.

(GE Healthcare, Sweden) by size-exclusion chromatography on a HiLoad 16/60 Superdex 30 or a HiPrep 16/60 Sephacryl S-200 HR column eluted with 1% BuOH in water at 1.0 mL min⁻¹.

Preparation of the O-deacetylated polysaccharide

The native PS (9.8 mg) was treated with aqueous 0.1 M NaOH (1 mL) at 25 °C for 15 h. The solution was then neutralized with a Dowex 50H⁺ resin, filtered, and lyophilized to yield O-deacetylated PS (6 mg, 62%). This material was further used for the preparation of the oligosaccharide material (see below). A similar O-deacetylated material (4.8 mg, used for the NMR analysis) was obtained after purification of the native PS (12.5 mg) by anion-exchange chromatography followed by desalting of the product by gel permeation chromatography (GPC). The anion exchange chromatography was performed on a HiTrap diethylaminoethyl (DEAE)-Sephacrose Fast Flow 5 mL column (GE Healthcare, Sweden) using 1% BuOH in water at 2 mL min⁻¹ for 7.5 column volumes, and eluted with the same solvent with a linear gradient (0 → 1 M aq NaCl over 5.5 column volumes). The GPC purification was performed on a HiLoad 16/60 Superdex 30 column eluted with 1% BuOH in water at 1.0 mL min⁻¹.

Preparation of the oligosaccharide material

The O-deacetylated PS (6 mg) was treated with 48% aq HF (3 mL) at 4 °C for 2 days and then at -22 °C for 2 days. After evaporation of the solvent with a stream of dry air, H₂O (2 mL) was added, and the solution was neutralized with 1 M aq NH₄OH; all these steps were carried out at 0 °C. The solution was then freeze-dried, and the product was purified by size-exclusion chromatography on a HiLoad 16/60 Superdex 30 column (GE Healthcare) eluted with 1% BuOH in water at 1.0 mL min⁻¹.

Mass spectrometry

The electrospray ionization high-resolution mass spectrum (ESI-HRMS) was recorded in positive mode using a MicrOTOF-QTM mass spectrometer (Bruker Daltonics). An MS/MS spectrum in positive mode was obtained from the *m/z* 983.4 ion precursor (sodium adduct) and a MS/MS spectrum in negative mode was obtained from the *m/z* 959.4 ion precursor [M-H]⁻. Nitrogen was used as the collision gas.

Sugar analysis and absolute configuration determination

The polysaccharide (0.3–0.5 mg) was hydrolyzed with 4 M aq HCl (0.3 mL) at 100 °C for 30 min. The sample was subsequently reduced with NaBH₄ and acetylated. The mixture of alditol acetates was analyzed by GLC. The absolute configuration of D-Glc, D-GlcNAc, D-GalNAc, and L-QuiNAc were determined by GLC analysis of their acetylated (+)-2-butyl glycoside derivatives.^[32]

GLC analysis

The alditol acetates and the acetylated butyl glycoside derivatives were separated on a PerkinElmer Elite-5 column with hydrogen as the carrier gas (25 psi) using a temperature program of 150 °C for 2 min, 3 °C min⁻¹ up to 220 °C, and then 10 min at 220 °C. The injector and detector temperatures were set to 220 and 250 °C, respectively. The acetylated butyl glycoside derivatives of *N*-acetylgalactosamine were separated on a PerkinElmer Elite-225 column with hydrogen as the carrier gas (25 psi) using a temperature program starting from 130 °C, 5 °C min⁻¹ up to 150 °C followed by 7 °C min⁻¹ up to 220 °C, and then 20 min at 220 °C. The injector and detector temperatures were set to 140 and 250 °C. The columns were fitted to a PerkinElmer Clarus 400 gas chromatograph equipped with flame ionization detectors. The retention times of the derivatives were compared with those of authentic reference compounds. The PS of *Proteus penneri* 26 was used as a reference compound for L-QuiN.^[33]

NMR spectroscopy

The NMR spectra were recorded on different spectrometers: Bruker Avance III 700 MHz equipped with a 5 mm TCI (¹H/¹³C/¹⁵N) Z-Gradient (53.0 G·cm⁻¹) CryoProbeTM, Bruker Avance III 600 MHz equipped with a 5 mm inverse Z-gradient (55.7 G·cm⁻¹) TXI probe (¹H/¹³C/³¹P), or Bruker Avance 500 MHz equipped with a 5 mm TCI (¹H/¹³C/¹⁵N) Z-Gradient (53.0 G·cm⁻¹) CryoProbe. Chemical shifts are reported in ppm using internal sodium 3-trimethylsilyl-(2,2,3,3-²H₄)-propionate (TSP, δ_H = 0.00 ppm), external 1,4-dioxane in D₂O (δ_C = 67.40 ppm), or 2% H₃PO₄ in D₂O (δ_P = 0.00 ppm) as references.

The NMR spectra of the oligosaccharide mixture (1 mg in 0.5 mL D₂O) were carried out on a 700 MHz spectrometer. The spectra of the native PS (2.6 mg in 0.5 mL D₂O) were also recorded on a 700 MHz spectrometer, with the exception of the ³¹P NMR-based experiments, which were carried out on a 600 MHz spectrometer (4.9 mg in 0.5 mL D₂O), and the spectra recorded on 95:5 H₂O:D₂O mixture, which were performed on a 500 MHz spectrometer. The NMR spectra of the O-deacetylated PS (4.8 mg in 0.6 mL D₂O) were recorded on a 500 MHz spectrometer, with exception of the ¹H spectra in Figure 1 and the multiplicity-edited ¹H,¹³C-HSQC spectrum of Figure 4a–c, which were recorded on a 600 MHz spectrometer.

The 1D diffusion-filtered ¹H NMR spectrum of Figure 1 was recorded using the 1D stimulated spin-echo pulse sequence with bipolar gradients (stebpgp2s1d).^[34] Diffusion encoded sinusoidal gradient pulses (δ/2) of 1.8 ms at 50% of the maximum strength were used;

the diffusion time was set to 200 ms. The $^1\text{H},^1\text{H}$ -TOCSY experiments were obtained using either an MLEV-17^[35] spin-lock of 10 kHz or a DIPSI-2^[36] spin-lock of 9.6 kHz and mixing times of 20, 40, 60, and 100 ms. The $^1\text{H},^1\text{H}$ -NOESY experiments^[37] were recorded with mixing times of 100 ms. The multiplicity-edited $^1\text{H},^{13}\text{C}$ -HSQC experiments^[38] were recorded employing the echo/antiecho method; adiabatic pulses^[39] were used for ^{13}C inversion (smoothed CHIRP, 20%, 80 kHz, 500 μs). The $^1\text{H},^{13}\text{C}$ -H2BC experiments^[40] were recorded with a constant-time delay of 22 ms. The gradient-selected $^1\text{H},^{13}\text{C}$ -HMBC experiments^[41] were carried out with evolution times of 50 ms in the case of the PSs and 63 ms in the case of the oligosaccharide. The $^1\text{H},^{13}\text{C}$ -band-selective constant-time HMBC ($^1\text{H},^{13}\text{C}$ -BS-CT-HMBC) experiments^[42] of the PSs were recorded over a spectral region of 6.0 ppm in the direct dimension and 9.0 ppm in the indirect dimension, with $2\text{k}\times 256$ data points and a delay for the evolution of the long-range couplings of 50 ms. A selective refocusing pulse (Q3 Gaussian cascade) of 2.5 ms was applied at the center of the region for the carbonyl carbons. The $^1\text{H},^{31}\text{P}$ -HMBC spectrum^[41,43] was recorded with an evolution time of 100 ms. The $^1\text{H},^{31}\text{P}$ -hetero-TOCSY experiments^[44] were carried out with mixing times of 23 and 46 ms, using a DIPSI-2^[36] mixing sequence set at 5.0 kHz on both channels. The $^1\text{H},^1\text{H}$ -TOCSY and $^1\text{H},^1\text{H}$ -NOESY spectra of the native PS dissolved in $\text{H}_2\text{O}:\text{D}_2\text{O}$ 95:5 mixture were recorded with water suppression by excitation sculpting^[45] using selective square pulses (Squa100.1000) of 2 ms.

Acknowledgements

This work was supported by grants from the Swedish Research Council and the Knut and Alice Wallenberg Foundation. This research has also received funding from the European Commission's Seventh Framework Programme FP7/2007–2013 under grant agreement no. 215536. The authors would like to thank the Swedish NMR Centre at Gothenburg University for granting NMR spectrometer time and Dr. Maxim Mayzel for his assistance in recording the experiments.

Keywords: *Escherichia coli* • NMR spectroscopy • O-antigen • polysaccharides • structure elucidation

- [1] J. B. Kaper, J. P. Nataro, H. L. Mobley, *Nat. Rev. Microbiol.* **2004**, *2*, 123–140.
- [2] J. P. Nataro, J. B. Kaper, *Clin. Microbiol. Rev.* **1998**, *11*, 142–201.
- [3] L. Beutin, *J. Vet. Med. Ser. B* **2006**, *53*, 299–305.
- [4] F. Ørskov, I. Ørskov, *Methods Microbiol.* **1984**, *14*, 43–112.
- [5] R. Stenutz, A. Weintraub, G. Widmalm, *FEMS Microbiol. Rev.* **2006**, *30*, 382–403.
- [6] Y. A. Knirel, in *Bact. Lipopolysaccharides. Struct. Chem. Synth. Biog. Interact. with Host Cells* (Eds.: Y. A. Knirel, M. A. Valvano), Springer, Vienna, **2011**, pp. 41–115.
- [7] S. Delannoy, L. Beutin, Y. Burgos, P. Fach, *J. Clin. Microbiol.* **2012**, *50*, 3485–92.
- [8] L. Beutin, S. Jahn, P. Fach, *J. Appl. Microbiol.* **2009**, *106*, 1122–1132.
- [9] T. Cheasty, *Culture* **2008**, *29*, 1–8.
- [10] M. Lundborg, V. Modhukur, G. Widmalm, *Glycobiology* **2010**, *20*, 366–368.
- [11] F. Scheutz, T. Cheasty, D. Woodward, H. R. Smith, *APMIS* **2004**, *112*, 569–584.
- [12] G. Buvens, D. Piérard, *Eur. J. Clin. Microbiol. Infect. Dis.* **2012**, *31*, 1463–1465.
- [13] C. García-Aljaro, M. Muniesa, J. E. Blanco, M. Blanco, J. Blanco, J. Jofre, A. R. Blanch, *FEMS Microbiol. Lett.* **2005**, *246*, 55–65.
- [14] M. Łopatek, K. Wiczorek, J. Osek, *Med. Weter.* **2012**, *68*, 488–492.
- [15] T. Rundlöf, A. Weintraub, G. Widmalm, *Carbohydr. Res.* **1996**, *291*, 127–39.
- [16] M. Linnerborg, A. Weintraub, G. Widmalm, *Carbohydr. Res.* **1999**, *320*, 200–208.
- [17] C. Landersjö, A. Weintraub, G. Widmalm, *Eur. J. Biochem.* **2001**, *268*, 2239–2245.
- [18] A. Dell in *Adv. Carbohydr. Chem. Biochem.* (Eds.: R. S. Tipson, D. Horton), Academic Press, Waltham, **1987**, *45*, pp. 19–72.
- [19] P.-E. Jansson, L. Kenne, G. Widmalm, *Carbohydr. Res.* **1989**, *188*, 169–191.
- [20] P. Söderman, P.-E. Jansson, G. Widmalm, *J. Chem. Soc. Perkin Trans. 2* **1998**, 639–648.
- [21] M. Lundborg, G. Widmalm, *Anal. Chem.* **2011**, *83*, 1514.
- [22] T. Yamagaki, H. Suzuki, K. Tachibana, *J. Am. Soc. Mass Spectrom.* **2006**, *17*, 67–74.
- [23] D. R. Bundle, R. U. Lemieux, *Methods Carbohydr. Chem.* **1976**, *7*, 79–86.
- [24] P.-E. Jansson, L. Kenne, E. Schweda, *J. Chem. Soc. Perkin Trans. 1* **1987**, 377–383.
- [25] J. Rönnols, R. Pendrill, C. Fontana, C. Hamark, T. Angles d'Ortoli, O. Engström, J. Ståhle, M. V. Zaccheus, E. Sävén, L. E. Hahn, S. Iqbal, G. Widmalm, *Carbohydr. Res.* **2013**, *380*, 156–166.
- [26] A. Ziolkowski, A. S. Shashkov, A. St. Sweierzko, S. N. Senchenkova, F. V. Toukach, M. Cedzynski, K.-I. Amano, W. Kaca, Y. A. Knirel, *FEBS Lett.* **1997**, *411*, 221–224.
- [27] S. N. Senchenkova, A. S. Shashkov, F. V. Toukach, A. Ziolkowski, A. S. Swierzko, K.-I. Amano, W. Kaca, Y. A. Knirel, N. K. Kochetkov, *Biochemistry (Moscow)* **1997**, *62*, 461–468.
- [28] L. Liao, V. Robertson, F.-I. Auzanneau, *Carbohydr. Res.* **2005**, *340*, 2826–2832.
- [29] B. Ruttens, R. Saksena, P. Kováč, *Eur. J. Org. Chem.* **2007**, 4366–4375.
- [30] A. Varki, R. D. Cummings, J. D. Esko, H. H. Freeze, P. Stanley, C. R. Bertozzi, G. W. Hart, M. E. Etzler, *Essentials of Glycobiology*, Cold Spring Harbor, New York, **2009**.
- [31] M. V. Svensson, A. Weintraub, G. Widmalm, *Carbohydr. Res.* **2011**, *346*, 449–453.
- [32] K. Leontein, J. Lönngren, *Methods Carbohydr. Chem.* **1993**, *9*, 87–89.
- [33] A. S. Shashkov, N. P. Arbatsky, G. Widmalm, Y. A. Knirel, K. Zych, Z. Sidorczyk, *Eur. J. Biochem.* **1998**, *253*, 730–733.
- [34] D. Wu, A. Chen, C. S. Johnson, *J. Magn. Reson. Ser. A* **1995**, *115*, 260–264.
- [35] A. Bax, D. G. Davis, *J. Magn. Reson.* **1985**, *65*, 355–360.
- [36] A. J. Shaka, C. J. Lee, A. Pines, *J. Magn. Reson.* **1988**, *77*, 274–293.
- [37] A. Kumar, R. R. Ernst, K. Wüthrich, *Biochem. Biophys. Res. Commun.* **1980**, *95*, 1–6.
- [38] J. Schleichner, M. Schwendinger, M. Sattler, P. Schmidt, O. Schedletsky, S. J. Glaser, O. W. Sørensen, C. Griesinger, *J. Biomol. NMR* **1994**, *4*, 301–306.
- [39] ě. Kupče, *Methods Enzymol.* **2002**, *338*, 82–111.
- [40] N. T. Nyberg, J. Ø. Duus, O. W. Sørensen, *J. Am. Chem. Soc.* **2005**, *127*, 6154–6155.
- [41] A. Bax, M. F. Summers, *J. Am. Chem. Soc.* **1986**, *108*, 2093–2094.
- [42] T. D. W. Claridge, I. Pérez-Victoria, *Org. Biomol. Chem.* **2003**, *1*, 3632–3634.
- [43] E. R. Zartler, G. E. Martin, *J. Biomol. NMR* **2011**, *51*, 357–367.
- [44] G. W. Kellogg, *J. Magn. Reson.* **1992**, *98*, 176–182.
- [45] T.-L. Hwang, A. J. Shaka, *J. Magn. Reson. Ser. A* **1995**, *112*, 275–279.

Received: September 18, 2014
 Published online on December 1, 2014